

# Nanoscale

Accepted Manuscript



This is an *Accepted Manuscript*, which has been through the Royal Society of Chemistry peer review process and has been accepted for publication.

*Accepted Manuscripts* are published online shortly after acceptance, before technical editing, formatting and proof reading. Using this free service, authors can make their results available to the community, in citable form, before we publish the edited article. We will replace this *Accepted Manuscript* with the edited and formatted *Advance Article* as soon as it is available.

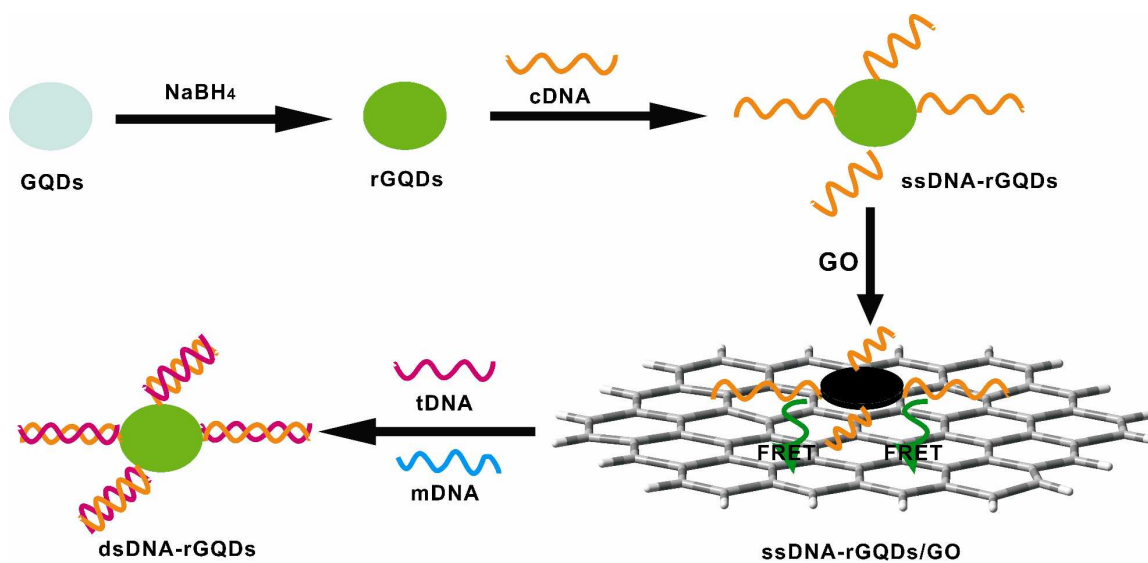
You can find more information about *Accepted Manuscripts* in the [Information for Authors](#).

Please note that technical editing may introduce minor changes to the text and/or graphics, which may alter content. The journal's standard [Terms & Conditions](#) and the [Ethical guidelines](#) still apply. In no event shall the Royal Society of Chemistry be held responsible for any errors or omissions in this *Accepted Manuscript* or any consequences arising from the use of any information it contains.

## Graphical Abstract

# A Universal Fluorescence Sensing Strategy Based on Biocompatible Graphene Quantum Dots and Graphene Oxide for Detection of DNA

Zhaosheng Qian, Xiaoyue Shan, Lujing Chai, Juanjuan Ma, Jianrong Chen and Hui Feng\*



A novel and efficient fluorescent sensing platform based on biocompatible graphene quantum dots and graphene oxide was established.

## COMMUNICATION

# A Universal Fluorescence Sensing Strategy Based on Biocompatible Graphene Quantum Dots and Graphene Oxide for Detection of DNA

Cite this: DOI: 10.1039/x0xx00000x

Z. S. Qian, X. Y. Shan, L. J. Chai, J. J. Ma, J. R. Chen and H. Feng\*

Received 00th January 2012,  
Accepted 00th January 2012

DOI: 10.1039/x0xx00000x

www.rsc.org/

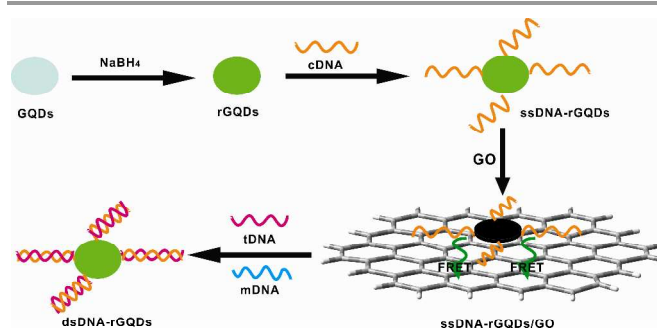
**A novel and efficient fluorescent sensing platform based on biocompatible graphene quantum dots and graphene oxide was established. It showed high selectivity and sensitivity for DNA detection.**

The presence and amount of biological markers including carbohydrates, proteins, DNA are often the important signal of some specific disease states and physiological processes, which has a unique advantage in accurate and sensitive warning of damage at low levels.<sup>1</sup> In disease diagnosis and medical fields, efficient and accurate identification and detection of these biological molecules at low cost is crucial.<sup>2</sup> Recently, based on the unique properties and excellent chemical sensing performance, a large number of nano materials were used to build simple biological nanosensors, which made good progress. Especially those nano-materials which have the unique optical absorption and fluorescence emission were widely applied to the detection of biological species.<sup>3</sup>

Fluorescence resonance energy transfer (FRET) which is known to be sensitive and reliable analytic method was widely used in biological analysis.<sup>4</sup> In order to improve the efficiency of fluorescence resonance energy transfer and analyze performance, it has always been an important work to find a suitable electron donor-acceptor pairs. In recent years, graphene attracted scientists' intense research interest because of its unique electronic, thermal, optical and mechanical properties.<sup>5</sup> It is found that graphene oxide (GO) can be used as the quenching agent to quench fluorescence of organic dyes since graphene oxide is a good electron acceptor in FRET, and thus many fluorescence sensing platforms for biological molecule detection were built based on graphene oxide.<sup>6</sup> Currently the fluorescent probes in biodetection are commonly organic dyes and inorganic semiconductor quantum dots (QDs). However, the dyes have shown some drawbacks such as poor photostability, easy photobleaching, small Stokes shifts and short lifetimes, while there are also great disadvantages of QDs because of their high toxicity, common blinking behavior and relatively high cost.<sup>7</sup> Since the discovery in 2004, graphene quantum dots (GQDs) have attracted wide attention of scientists in different fields due to their unique properties and excellent

performance in photovoltaic devices, photocatalysis and biological imaging.<sup>8</sup> Particularly, due to their outstanding fluorescence performance, GQDs have shown promising application prospect in bioimaging and biodetection.<sup>9</sup> Compared with conventional dye molecules and semiconductor QDs, GQDs have great superiorities including low toxicity, excellent biocompatibility, good resistance to photobleaching, stable emission and easy modulation.<sup>10</sup> Therefore, GQDs are expected to be the outstanding alternative instead of organic dyes and semiconductor QDs for fluorescence sensing platform.

In this communication, a highly selective and sensitive fluorescence sensing approach for DNA detection based on biocompatible graphene quantum dots and graphene oxide was established. We take advantage of good biocompatibility and strong fluorescence of GQDs, base pairing specificity of DNA and unique fluorescence resonance energy transfer between GQDs and GO to achieve quantitative analysis of DNA. Scheme 1 shows the schematic illustration of DNA detection strategy based on FRET between rGQDs labeled DNA probe and GO. The rGQDs with strong fluorescence were obtained by reduction of GQDs with NaBH<sub>4</sub> first. The detection of target DNA is accomplished by following three steps: in the first step, single-stranded DNA probe (ssDNA-rGQDs) was prepared with connecting DNA (cDNA) and rGQDs through



**Scheme 1** Schematic illustration of a universal fluorescent sensing platform for detection of DNA based on fluorescence resonance energy transfer (FRET) between graphene quantum dots and graphene oxide.

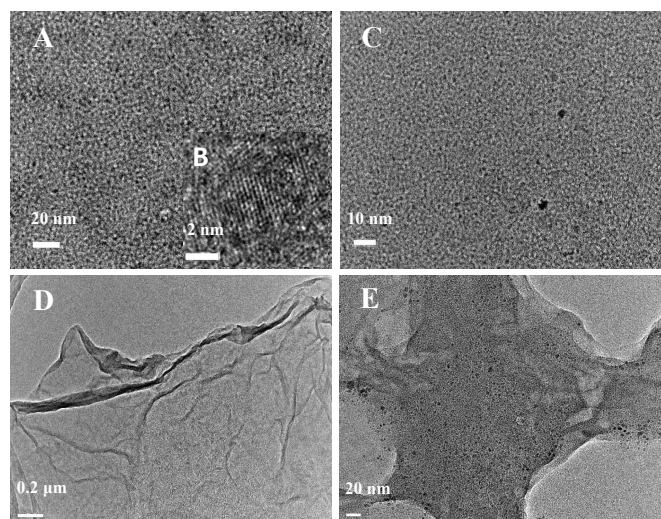


**Fig. 1** The TEM images of as-prepared rGQDs (A), ssDNA-rGQDs (C), GO (D), ssDNA-rGQDs + GO (E) and HRTEM image of rGQDs (B).

condensation; Then, ssDNA-rGQDs probe was absorbed on the surface of GO through electrostatic attraction and  $\pi$ - $\pi$  stacking interactions, leading to substantial fluorescence quenching. In the third step, DNA hybridization between ssDNA-GQDs and target DNA (tDNA) leads to dsDNA-GQDs which are detached and thus liberated from GO, resulting in fluorescence recovery. Upon the addition of tDNA, tDNA can capture ssDNA-GQDs in the assembly ssDNA-rGQDs/GO to produce the dsDNA-rGQDs through specific base pairing. The formation of dsDNA-rGQDs breaks up electrostatic attraction and  $\pi$ - $\pi$  stacking interaction between ssDNA-rGQDs and GO, and thus leads to liberation and detachment of dsDNA-rGQDs from GO, resulting in fluorescence recovery from free dsDNA-GQDs.

The pristine GQDs were synthesized from graphite powder through oxidation with mixed  $\text{H}_2\text{SO}_4$  and  $\text{HNO}_3$  and further neutralization with sodium hydroxide. The as-prepared GQDs were reduced by sodium borohydride to obtain reduced GQDs (rGQDs). Both GQDs and rGQDs were dialyzed to remove the extra original compounds and produced salts. The transmission electron microscopy (TEM) image in Fig. 1A showed the average size of rGQDs is about  $5 \pm 3$  nm. High resolution transmission electron microscopy (HRTEM) image in Fig 1B depicted the graphene-like crystalline structure of GQDs, and the spacing of adjacent lattice planes spans from  $3.0 \pm 0.2$  Å, which is close to data of GQDs reported in reference and consistent with (002) diffraction plane of graphite.<sup>11</sup> The XPS spectra showed both GQDs and rGQDs mainly consist of carbon (at ca. 284.8 eV) and oxygen (at ca. 531.4 eV) as shown in Fig. S1. Except for carbon and oxygen, a certain amount of sodium was also observed owing to remaining sodium salts. The harsh treatment of combined sulfuric acid and nitric acid cleaved graphite into nanodots with oxygen-rich surface groups including hydroxyl, carbonyl, carboxyl and epoxy. This is verified by high content of oxygen (63.52%) for GQDs in Table S1 and XPS C1s core lines from C=O (288.6) and C-O (286.6) in Fig S2.<sup>12,13</sup> The reduction by  $\text{NaBH}_4$  can selectively reduce the carbonyl and epoxy moieties to hydroxyl groups and remain other functional groups (C=C and COOH). After reduction rGQDs possess lower oxygen content with 60.79% than GQDs. Comparison of XPS C1s spectra between GQDs and rGQDs clearly demonstrated that C-O peak at 286.6 eV obviously enhanced in intensity after reduction (Fig. S2). This is also

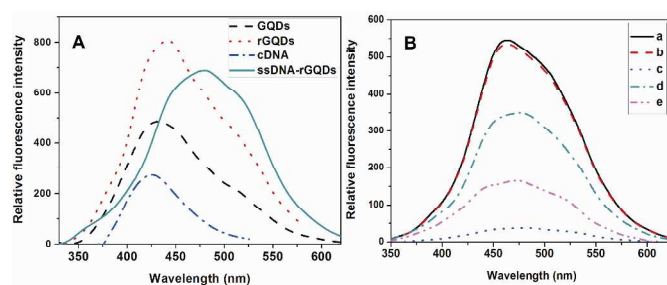


**Fig. 2** The fluorescence spectra of GQDs, rGQDs, cDNA and ssDNA-rGQDs (A), and fluorescence change of the species (B). (a) ssDNA-rGQDs (black line), (b) ssDNA-rGQDs + 100.0 nM tDNA (red line), (c) ssDNA-rGQDs +  $28.0 \mu\text{g mL}^{-1}$  GO (blue line), (d) ssDNA-rGQDs +  $28.0 \mu\text{g mL}^{-1}$  GO + 100.0 nM tDNA (green line) and (e) ssDNA-rGQDs +  $28.0 \mu\text{g mL}^{-1}$  GO + 100.0 nM mDNA (pink line).

verified by the apparent increase of vibrational absorption bands of  $1140 \text{ cm}^{-1}$  from C-O and  $3437 \text{ cm}^{-1}$  from O-H upon the reduction of GQDs (Fig. S3). rGQDs exhibit bright blue fluorescence centered at 443 nm in water under UV light, whereas GQDs show weak light at 430 nm as shown in Fig. 2A. The PL quantum yield of rGQDs is up to 20.4%, much higher than that of GQDs (1.7%) (Table S2), suggesting great enhancement of fluorescence upon the reduction. GO was synthesized from graphite powder based on a modified Hummer's method.<sup>14</sup> As-prepared GO was readily water-dispersible due to the presence of suspended hydroxyl and carboxylic groups at the surface. TEM image in Fig.1D clearly showed the characteristic morphology of GO.

We evaluated the feasibility of combined rGQDs and GO as a fluorescent sensing platform for DNA detection with the use of an oligonucleotide sequence associated with human cancer gene as a model system. The rGQDs-labeled single-stranded DNA probe, ssDNA-rGQDs, was prepared using connecting DNA (cDNA) and rGQDs through condensation reaction. Fig. 2A displayed distinctive fluorescence emission of ssDNA-rGQDs from those of rGQDs and cDNA, providing the evidence for successful synthesis of DNA probe. The fluorescence of ssDNA-rGQDs is shifted to 480 nm with strong green color owing to functionalized cDNA (Fig 2B curve a). However, the presence of  $28.0 \mu\text{g mL}^{-1}$  GO results in nearly absolute fluorescence quenching of the probe (curve c), indicating that the GO can adsorb ssDNA-rGQDs and quench its fluorescence very effectively. This point was verified by the TEM image of ssDNA-rGQDs and GO mixture in Fig 1E, which clearly demonstrated that the probes were adsorbed on surface of GO. Upon its incubation with complementary target tDNA over a 30 minutes' period, the mixture exhibits significant fluorescence enhancement, leading to 70% fluorescence recovery (curve d). This recovery is due to the separation of double-stranded DNA-rGQDs (dsDNA-rGQDs) formed between ssDNA-rGQDs probe and tDNA from GO surface. While, when the target DNA was replaced by single-base mismatched DNA (mDNA), the recovered fluorescence is much weaker than that from tDNA (curve e), suggesting the good selectivity of the approach. It should be pointed out that the fluorescence of ssDNA-GQDs probe was scarcely influenced by the addition of tDNA in the absence of GO (curve b). In addition, GO itself exhibits no fluorescence emission, which makes no contribution to whole fluorescence intensity of each sample measured.

This unique fluorescence "on-off-on" process based on rGQDs and GO can serve as a sensitive sensing system for quantitative DNA analysis. In order to develop this analytical

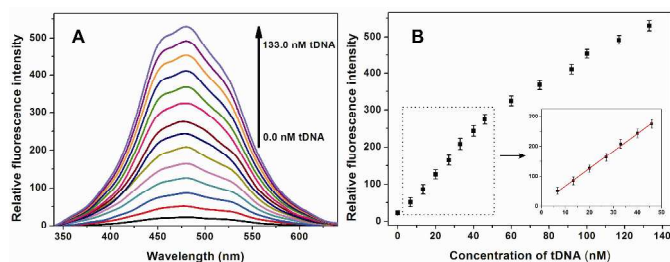


**Fig. 3** (A) The fluorescence recovery of ssDNA-rGQDs/GO system after incubation with various concentrations of tDNA (0.0, 6.7, 13.3, 20.0, 27.0, 33.0, 40.0, 46.0, 75.0, 92.0, 100.0, 117.0, 133.0 nM), (B) The linear relationship between the fluorescence intensity and concentration of tDNA.

method, optimal conditions including concentration of added GO, incubation time of fluorescence quenching and recovery were investigated. Fig S4 shows quenching efficiency dependent on concentration of GO, and  $16.0 \mu\text{g mL}^{-1}$  as the optimal concentration of GO was chosen. Fig S5 displays the quenching effect as a function of incubation time. One can note that quenching effect remains nearly constant after 30 minutes. The optimal time of fluorescence recovery was also optimized as shown in Fig S6, in which the curve shows a rapid growth in the first 20 minutes, and then keeps identical after 30 minutes. Thus, both the optimal fluorescence quenching time and recovery time were chosen as 30 minutes.

Under the optimal conditions, the sensing performance of this system was evaluated by adding varying concentrations of tDNA into the proceeding ssDNA-rGQDs/GO solution. The fluorescence comes from dsDNA-rGQDs formed between ssDNA-rGQDs and tDNA after addition of tDNA into ssDNA-rGQDs/GO system. As illustrated in Fig. 3A, fluorescence intensity of dsDNA-rGQDs was increased gradually after addition of increased concentrations of tDNA because more and more amounts of dsDNA-rGQDs formed and escaped from GO surface. The linear relationship between fluorescence intensity and concentration of tDNA shown in Fig. 3B was established, and can be expressed as  $y = 5.78x + 11.13$ , where  $R^2 = 0.998$ . The established method for DNA detection has a broad linear range of 0.0 – 46.0 nM with a detection limit of 75.0 pM DNA as estimated from the derived calibration curve ( $>3$  standard deviations). This is the first time to achieve sensitive detection of DNA based on GQDs and GO platform to our best knowledge. This reported DNA detection approach possesses superiorities in linear range and detection limit relative to GO-based DNA platform reported by Lu et al.<sup>15</sup> Compared with DNA nanosensor based on graphene and FAM-tagged probe reported by He et al.,<sup>16</sup> the DNA nanosensor in this work has broader linear range, lower detection limit, and comparable assay time (less than 30 minutes).

In summary, a novel and effective fluorescent sensing platform for detection of DNA has been established based on FRET through regulating the interaction between GO and GQDs for the first time. It can be served as a universal strategy for DNA detection. This sensing system can distinguish complementary and mismatched nucleic acid sequences with high sensitivity and good reproducibility. Since all the materials involved in the sensing system are of excellent biocompatibility, it is expected that this DNA detection method would be used in vivo and in vitro, and promote the application of carbon-based nanomaterials in immunoassays.

We are thankful for the support by the National Natural Science Foundation of China (No. 21005073, 21275131,

21275130 and 21175118) and Zhejiang Province (No. LY13B050001, LQ13B050002 and 2011C3751).

## Notes and references

College of Chemistry and Life Science, Zhejiang Normal University, Jinhua 321004, China. Fax: +86-579-82282269; Tel: +86-579-82282269; E-mail: jenghui@zjnu.cn.\* Corresponding authors.

† Electronic Supplementary Information (ESI) available: XPS, FTIR spectra and experimental details. See DOI: 10.1039/b000000x/

- C. C. You, O. R. Miranda, B. Gider, P. S. Ghosh, I. Kim, B. Erdogan, S. A. Krovi, U. H. F. Bunz and V. M. Rotello, *Nat. Nanotechnol.*, 2007, **2**, 318; U. H. Bunz and V. M. Rotello, *Angew. Chem. Int. Ed.*, 2010, **49**, 3268.
- B. B. Haab, *Curr. Opin. Biotechnol.*, 2006, **17**, 415.
- X. Q. Chen, Y. Zhou, X. J. Peng and J. Y. Yoon, *Chem. Soc. Rev.*, 2010, **39**, 2120; K. Zhang, H. B. Zhou, Q. S. Mei, S. H. Wang, G. J. Guan, R. Y. Liu, J. Zhang and Z. P. Zhang, *J. Am. Chem. Soc.*, 2011, **133**, 8424; M. Y. Han, X. H. Gao, J. Z. Su and S. Nie, *Nat. Biotechnol.*, 2001, **19**, 631.
- E. A. Jares-Erijman and T. M. Jovin, *Nat. Biotechnol.*, 2003, **21**, 1387; B. Schuler and W. A. Eaton, *Curr. Opin. Struct. Biol.*, 2008, **18**, 16.
- X. Huang, X. Y. Qi, F. Boey and H. Zhang, *Chem. Soc. Rev.*, 2012, **41**, 666; X. Huang, Z. Y. Yin, S. X. Wu, X. Y. Qi, Q. Y. He, Q. C. Zhang, Q. Y. Yan, F. Boey and H. Zhang, *Small*, 2011, **7**, 1876. X. L. Li, X. R. Wang, L. Zhang, S. Lee and H. J. Dai, *Science*, 2008, **319**, 1229; D. Tasis, N. Tagmatarchis, A. Bianco, M. Prato, *Chem. Rev.*, 2006, **106**, 1105; N. Karousis, N. Tagmatarchis and D. Tasis, *Chem. Rev.*, 2010, **110**, 5366.
- C.-H. Lu, H.-H. Yang, C.-L. Zhu, X. Chen, G.-N. Chen, *Angew. Chem. Int. Ed.*, 2009, **48**, 4785; N. Mohanty and V. Berry, *Nano Lett.*, 2008, **8**, 4469; R. H. Yang, Z. W. Tang, J. L. Yan, H. Z. Kang, Y. M. Kim, Z. Zhu and W. H. Tan, *Anal. Chem.*, 2008, **80**, 7408; H. L. Li, J. Q. Tian, L. Wang, Y. W. Zhang and X. P. Sun, *J. Mater. Chem.*, 2011, **21**, 824.
- X. Q. Wu, H. J. Liu, J. Q. Liu, K. N. Haley, J. A. Treadway, J. P. Larson, N. F. Ge, F. Peale and M. P. Bruchez, *Nat. Biotechnol.*, 2003, **21**, 41; M. Howarth, W. Liu, S. Puthenveetil, Y. Zheng, L. F. Marshall, M. M. Schmidt, K. D. Wittrup, M. G. Bawendi, A. Y. Ting, *Nat. Methods*, 2008, **5**, 397; X. Michalet, F. F. Pinaud, L. A. Bentolila, J. M. Tsay, S. Doose, J. J. Li, G. Sundaresan, A. M. Wu, S. S. Gambhir, S. Seiss, *Science*, 2005, **307**, 538; R. C. Somers, M. G. Bawendi and D. G. Nocera, *Chem. Soc. Rev.*, 2007, **36**, 579.
- V. Gupta, N. Chaudhary, R. Srivastava, G. D. Sharma, R. Bhardwaj and S. Chand, *J. Am. Chem. Soc.*, 2011, **133**, 9960; X. Yan, X. Cui, B. S. Li and L. S. Li, *Nano Lett.*, 2010, **10**, 1869.
- Z. Lin, W. Xue, H. Chen and J.-M. Lin, *Anal. Chem.*, 2011, **83**, 8245; H. X. Zhao, L. Q. Liu, Z. D. Liu, Y. Wang, X. J. Zhao and C. Z. Huang, *Chem. Commun.*, 2011, **47**, 2604; W. Shi, X. H. Li and H. M. Ma, *Angew. Chem. Int. Ed.*, 2012, **51**, 6432; J. Zhao, G. F. Chen, L. Zhu and G. X. Li, *Electrochem. Commun.*, 2011, **13**, 31.
- L. Cao, X. Wang, M. J. Mezziani, F. S. Lu, H. F. Wang, P. G. Luo, Y. Lin, B. A. Harruff, L. M. Veca, D. Murray, S. Y. Xie and Y.-P. Sun, *J. Am. Chem. Soc.*, 2007, **129**, 11318; S.-T. Yang, L. Cao, P. G. Luo, F. S. Lu, X. Wang, H. F. Wang, M. J. Mezziani, Y. F. Liu, G. Qi and Y.-P. Sun, *J. Am. Chem. Soc.*, 2009, **131**, 11308.

## COMMUNICATION

- 11 Z. Qian, J. Ma, X. Shan, L. Shao, J. Zhou, J. Chen and H. Feng, *RCS Adv.* 2013, **3**, 14571; H. T. Li, X. D. He, Z. H. Kang, H. Huang, Y. Liu, J. L. Liu, S. Y. Lian, C. H. A. Tsang, X. B. Yang and S.-T. Lee, *Angew. Chem. Int. Ed.*, 2010, **49**, 4430;
- 12 J. F. Moulder, W. F. Stickle, P. E. Sobel and K. D. Bomben. Handbook of X-Ray photoelectron spectroscopy-A reference book of standard spectra for identification and interpretation of XPS data (Perkin-Elmer Corporation, Eden Prairie, MN, USA, 1992).
- 13 H. Z. Zheng, Q. L. Wang, Y. J. Long, H. J. Zhang, X. X. Huang and R. Zhu, *Chem. Commun.*, 2011, **47**, 10650.
- 14 W. Hummers and J. Offeman, *J. Am. Chem. Soc.* 1958, **80**, 1339; Y. Q. Wen, F. F. Xing, S. J. He, S. P. Song, L. H. Wang, Y. T. Long, D. Li and C. H. Fan, *Chem. Commun.*, 2010, **46**, 2596.
- 15 C. H. Lu, H. H. Yang, C. L. Zhu, X. Chen and G. N. Chen, *Angew. Chem. Int. Ed.*, 2009, **48**, 4787.
- 16 S. J. He, B. Song, D. Li, C. F. Zhu, W. P. Qi, Y. Q. Wen, L. H. Wang, S. P. Song, H. P. Fang and C. H. Fan, *Adv. Funct. Mater.*, 2010, **20**, 453.